The Astrophysical Journal, 820:64 (5pp), 2016 March 20 doi:10.3847/0004-637X/820/1/64

TEMPORAL EVOLUTION OF THE VELA PULSAR'S PULSE PROFILE

J. L. Palfreyman[1], J. M. Dickey[1], S. P. Ellingsen[1], I. R. Jones[1], and A. W. Hotan[2]
[1] Department of Physical Sciences, University of Tasmania, Private Bag 37, Hobart, Tasmania 7001, Australia; jim77742@gmail.com
[2] CSIRO Astronomy and Space Science, 26 Dick Perry Avenue, Technology Park, Kensington WA 6151, Australia
Received 2015 October 18; accepted 2016 February 4; published 2016 March 18

ABSTRACT

The mechanisms of emission and changes in rotation frequency ("glitching") of the Vela pulsar (J0835−4510) are not well understood. Further insight into these mechanisms can be achieved by long-term studies of integrated pulse width, timing residuals, and bright-pulse rates. We have undertaken an intensive observing campaign of Vela and collected over 6000 hr of single-pulse data. The data shows that the pulse width changes with time, including marked jumps in width after micro-glitches (frequency changes). The abundance of bright pulses also changes after some micro-glitches, but not all. The secular changes in pulse width have three possible cyclic periods that match with X-ray periodicities of a helical jet that are interpreted as free precession.

Key words: pulsars: general – pulsars: individual (PSR J0835−4510) – radiation mechanisms: non-thermal

1. INTRODUCTION

The Vela pulsar (J0835−4510) has been the focus of many studies. Much of this has focused on either long-term timing (e.g., Dodson et al. 2007) or short-term single pulse studies (e.g., Johnston et al. 2001). Here we report on both a long-term and single-pulse study of the Vela pulsar.

Vela is a young, close, and bright pulsar with characteristic age $\tau_c = 11.3$ kyr, distance $D \approx 280$ pc, flux $S_{1400} = 1100$ mJy (Manchester et al. 2005), making it a good candidate for studies using medium-sized radio telescopes. Vela regularly "glitches" or speeds up in rotation frequency ν with $\Delta\nu/\nu \approx 2000$–$3000 \times 10^{-9}$ (Radhakrishnan & Manchester 1969; Reichley & Downs 1969).

Dodson et al. (2007) have previously demonstrated that Vela glitches approximately every three years. Micro-glitches, as defined by Cordes et al. (1988) as $\Delta\nu/\nu \lesssim 1000 \times 10^{-9}$, also typically occur a number of times per year (D'Alessandro 1995).

Giant pulses are considered as ones that have mean flux densities of at least 10 times the average pulse. Johnston et al. (2001) reported "giant micro-pulses" and Palfreyman et al. (2011) showed that Vela has bright pulses (five times the average pulse) and consecutive bright pulses. No genuine giant pulses have been mentioned in the literature.

Vela's integrated pulse profile is well-known to change with frequency (Cordes 1978), but despite the variation in the brightness of individual pulses, there has been minimal mention in the literature of pulse profile changes in Vela over time at a fixed frequency. The exception is Cordes (1993) where a single tantalizing sentence mentions a pulse shape variability in the Vela profile with a period of 100 days.

In this paper we show that not only does Vela's pulse width change over time, it changes sharply after a micro-glitch, and that the rate of bright-pulse activity also changes with micro-glitches. We also show that the profile changes have three quasi-periodic components (one of which has a period of ≈100 days) that match with periods found in X-ray observations of a helical jet by Durant et al. (2013).

2. OBSERVATIONS AND DATA REDUCTION

In 2014 March we commenced a long-term single-pulse study of the Vela pulsar, collecting up to 19 hr of data each day. After 18 months we have collected over 6000 hr of single-pulse data.

We used the Mt Pleasant 26 m radio telescope (see Table 1) with a center frequency of 1376 MHz and a bandwidth of 64 MHz. The receiver consists of a 20 cm prime-focus feed-horn with cooled dual linear polarization feeds that are sampled with 2 bit precision at 128 million samples per second.

Each 10 s "raw" baseband file is 640 MB in size producing 4 TB of data each day. The data is then folded and phase-coherently de-dispersed using DSPSR (van Straten & Bailes 2011) with 16 frequency channels and 8192 pulse phase bins giving a time resolution of 10.9 μs. Currently, raw files containing "interesting" events are retained, with the remainder being discarded after about six months. All of the data is stored on the local RDSI 2.3 PB storage facility for later analysis using PSRCHIVE (Hotan et al. 2004).

Each file was folded in frequency, polarization, and time, then matched to a fixed standard profile template to produce a time of arrival. Residuals for the day were then calculated using TEMPO2 (Hobbs et al. 2006) and bad timing data—typically caused by radio frequency interference (RFI) or wind stows—were removed. A best fit of ν and $\dot{\nu}$ was performed producing a residual plot appearing as white noise with a typical rms of ≈50 μs. Finally, all of the day's 10 s files were phase aligned and integrated using the ν and $\dot{\nu}$ just calculated. A successful full day's observing of 19 hr would produce an integrated profile from over 7.5×10^5 individual pulses and have a signal-to-noise ratio (S/N) of around 2×10^4. Days that were shortened ($\lesssim$3 hr) due to other observers or wind stows were removed from the analysis.

The arrival time residuals of these daily integrated profiles were then used to search for micro-glitches. The PSRCHIVE utility "pdv" was used to produce the pulse widths at 10% and 50% of the pulse heights of the integrated profile. We developed an algorithm to select a pulse as being "bright" but yet not including any RFI that passed through the timing residual stage if the following two conditions were met.

1. The pulse has a peak flux of 10 or more times the average pulse.
2. The pulse at the 50% level has a width (FWHM) of between ≈160 and 550 μs (15–50 timing bins).

Table 1
Receiving System, Sampling, and Data Collected

Component	Parameter	Value
Telescope	Diameter (m)	26
Location	WGS84	
	Longitude	147°26′25.″87 E
	Latitude	42°48′12.″90 S
	Altitude (m)	65.09
Receiver	Frequency (MHz)	1376
	Bandwidth (MHz)	64
	Feeds	Dual Cooled
	Polarization	Linear
	SEFD (Jy)	500
Sampling	System	LBA DAS
	Bits	2
	Rate (MS s^{-1})	128
	File size (s)	10
Processing	Frequency channels	16
	Phase bins	8192
	Resolution (μs)	10.9
Data collected	Hours	6000
	Single pulses	237×10^6
	Disk usage (PB)	1.5

To confirm the algorithm's effectiveness, we manually checked all 41,442 bright pulses to verify how many were actually RFI. Only ≈5% were falsely selected by the algorithm and these were removed from the analysis.

3. PULSE SHAPE CHANGES

Figure 1 shows a plot of the 50% and 10% profile widths, timing residuals, and bright-pulse rate for MJD 56746 to 57281. At MJD = 57143 a micro-glitch of magnitude $\Delta\nu/\nu = 75.6 \times 10^{-9}$ occurred (see Figure 2), and a noticeable and sustained reduction in the pulse width at both 50% and 10% of the pulse height can be seen.

Jankowski et al. (2015) reported a micro-glitch at MJD = 56922 with a magnitude of $\Delta\nu/\nu = 0.4 \times 10^{-9}$ (see Figure 3). This coincided with a large increase in bright-pulse activity.

The plot of the pulse width over a year shows distinct cyclical variations on the order of 20–30 μs. Figure 4 shows a Lomb–Scargle periodogram (Lomb 1976; Scargle 1982), which has significant ($p = 0.001$) period peaks at 78 ± 5, 100 ± 7, and 137 ± 12 days.

We also found a strong correlation ($r = 0.914$) between the pulse widths at 10% and 50% of the peak (see Figure 5) through the entire data set.

This implies that what is affecting the pulse width is affecting the entire pulse shape.

Our observations show that after the second and larger micro-glitch the pulse has decreased in width by about 40 μs (2.6%) at the 50% level and about 60 μs (1.7%) at the 10% level.

Note that even though we observed with a bin width of 10.9 μs, we have from Lorimer & Kramer (2004):

$$\sigma_T \approx \frac{W}{\mathrm{S/N}} = \frac{5\ \mathrm{ms}}{20000} = 0.250\ \mu\mathrm{s}, \quad (1)$$

where σ_T is the timing error, W is the pulse width, and S/N is the signal-to-noise ratio. This shows that the error bars in Figures 1(a)–(c) would be smaller than the plotted points after integrating over 19 hr.

Pulse profile width changes like this could be caused by a slight change in our sight line to the pulsar's magnetic axis β (see Figure 6) both generally throughout the year and also a step change associated with the micro-glitch. For this to happen, either a change in the pulsar's rotational axis relative to the Earth (geodetic precession) or a change in the magnetic axis angle (α) relative to the rotational axis (free precession) has occurred.

Precession of the Vela pulsar has been raised in the literature previously. Durant et al. (2013) reveal a helical X-ray jet streaming from the rotational axis of the Vela pulsar potentially caused by precession. The jet has "acceptable" periods of 122 ± 5, 73 ± 2, or 91 ± 5 days. We see three definite periods in our pulse width data whose ranges fall within the "acceptable" periods mentioned in Durant et al. as shown by Figure 7.

Stairs et al. (2000) also discuss precession in a different pulsar (J1830−1059) and the periodicity in their timing residuals is very clear. However, J1830−1059 does not glitch like Vela so the cycles are easy to measure over a long period of time. They conclude that precession is the simplest explanation for their observations.

The change in α for Vela has also been discussed by Link & Epstein (1997). They contend that its very low braking index of 1.4 ± 0.2 is caused by an increase of α over time. For Vela, $\alpha = 55°$ and $\beta = -6°$ (Johnston et al. 2001), so since β is negative we have an inside sight line (see Figure 6). An increase in α implies the pulse width should be shrinking overall. Our data shows a pattern of pulse width increase and then decrease following the small micro-glitch at MJD = 56922. After the much larger micro-glitch at MJD = 57143, we see a sharp decrease in pulse width followed by a steady increase.

Link & Epstein (1997) also state that the evolution of α is not monotonic and that it seems to be different with older pulsars as compared with younger ($t_{\mathrm{age}} \lesssim 10^4$ years) ones.

Profile width changes could also be caused by a change in the width of the emission cone (ρ). This has been discussed in Rankin (1993) which shows a link between the conal width and the pulse period: the slower the pulsar, the narrower the emission cone. Now since a glitch is a fractional increase in rotation frequency, this would imply a widening of the emission cone. With the larger micro-glitch, we observed a sharp decrease followed by a slow increase in the pulse width. Regardless, the rotational increase is so small that Rankin's relation ($W = 5.°8P^{-1/2}$) predicts a pulse width change of only 0.178 ns. Of interest is that changes in emission cone width are linked to rotational frequency and that a micro-glitch could be linked to a change in the pulse width.

There are three distinct visible and one non-visible features in the integrated profile of the Vela pulsar (see Figure 8):

a. a large main peak,
b. a "ledge" to the right,
c. a gentle point of inflection, and
d. a bright-pulse emission zone.

Krishnamohan & Downs (1983) discuss these four pulse components, their distributions, and their emission heights.

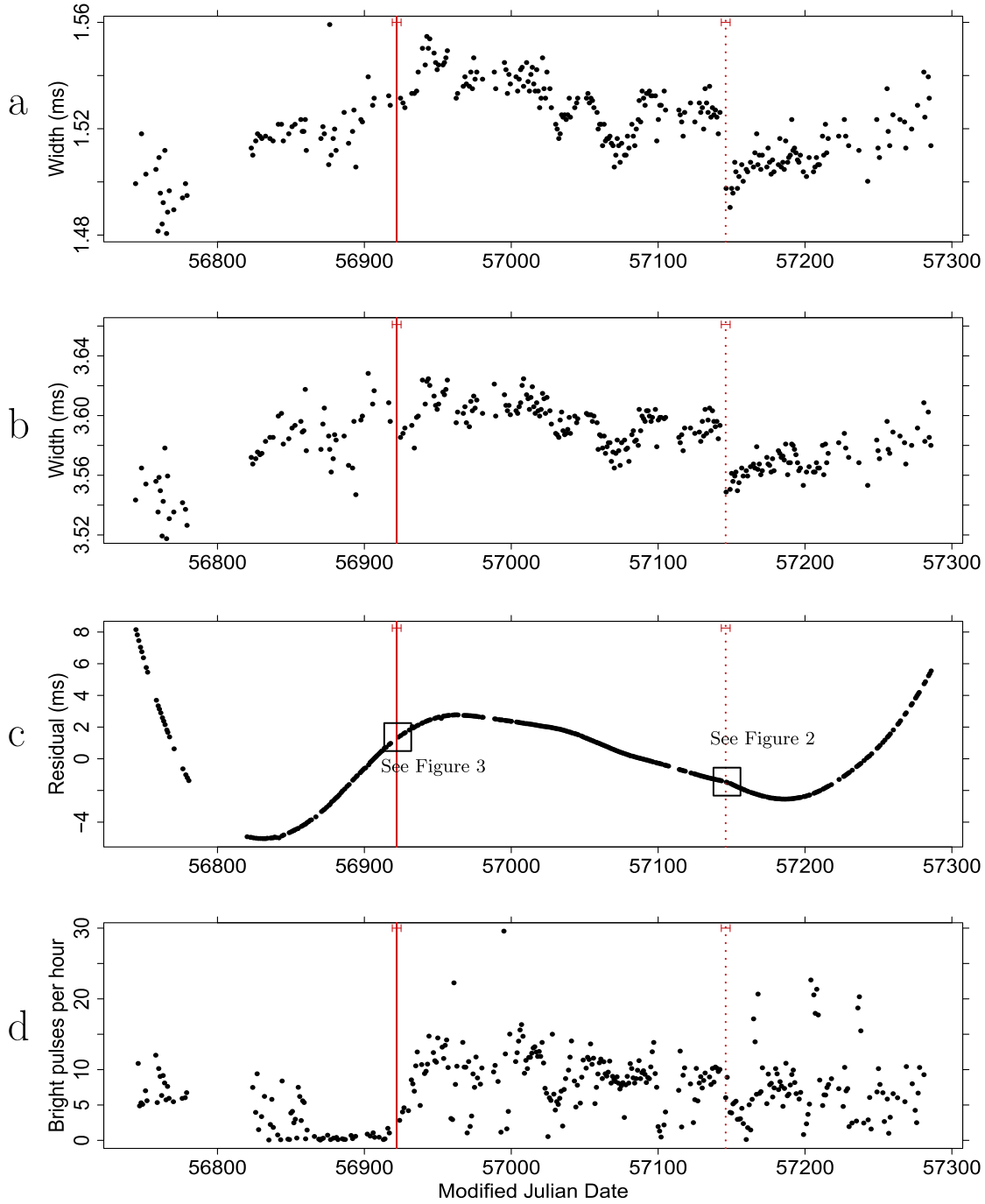

Figure 1. (a) Plot of pulse width (in ms) at 50% of the peak of the integrated pulse, (b) the pulse width at 10% of the peak, (c) the timing residuals, and (d) the bright-pulse rate. Note the sudden decrease in both pulse widths when the magnitude $\Delta\nu/\nu = 75.6 \times 10^{-9}$ micro-glitch at MJD = 57143 occurred (dotted line). Note the 50 day quiet period and then sudden increase in bright-pulse rate after the first glitch of magnitude $\Delta\nu/\nu = 0.4 \times 10^{-9}$ that occurred at MJD = 56922 (solid line). Each dot is a day of observing and all errors bars are smaller than the dots.

The leading edge bright-pulse component (*d*) is not visible in the integrated profile because it only appears rarely. However, when the pulsar does emit a bright pulse, it is always on the leading edge and it affects the pulse width strongly at both the 10% and 50% levels. Therefore, an increase in bright-pulse rates should positively correlate with an increase in the pulse width. It can be seen this is the case around the first small micro-glitch (MJD = 56922), but it is clearly not the case with the large micro-glitch (MJD = 57143) where the sudden decrease in the pulse width did not appear alongside a sudden drop in the bright-pulse rate. A Lomb–Scargle periodogram of the bright-pulse rates shows no significant periodicities.

This is a paradox. The first micro-glitch coincides with a sudden increase in the bright-pulse rates with no apparent change in the pulse width. The second micro-glitch coincides with a sudden decrease in the pulse width with no apparent change in the bright-pulse rate.

This can be explained in the model of Wright (2003), who considers that emission zones might be mathematically chaotic in nature; however, this hypothesis relies on the emission zones

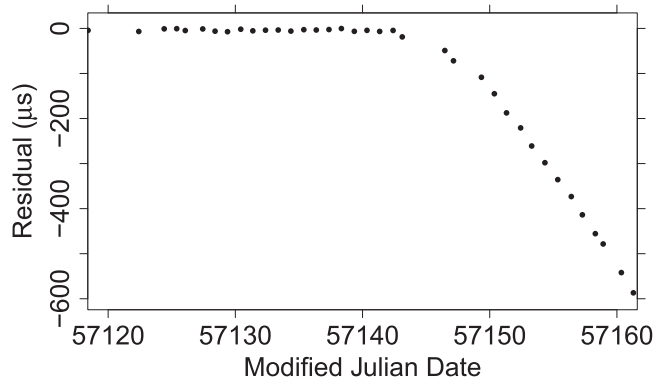

Figure 2. Daily timing residuals showing the $\Delta\nu/\nu = 75.6 \times 10^{-9}$ mag micro-glitch at MJD $= 57143 \pm 3$.

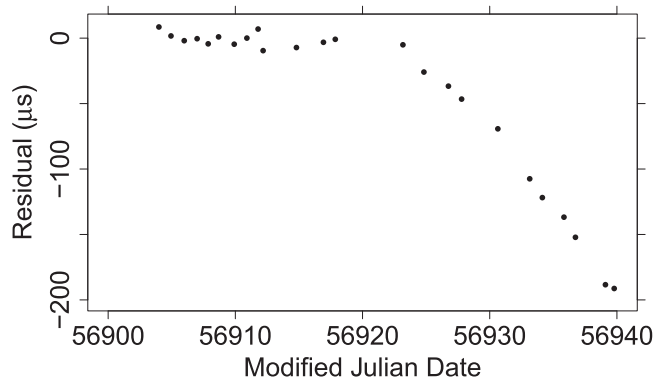

Figure 3. Daily timing residuals showing the $\Delta\nu/\nu = 0.4 \times 10^{-9}$ mag micro-glitch at MJD $= 56922 \pm 3$.

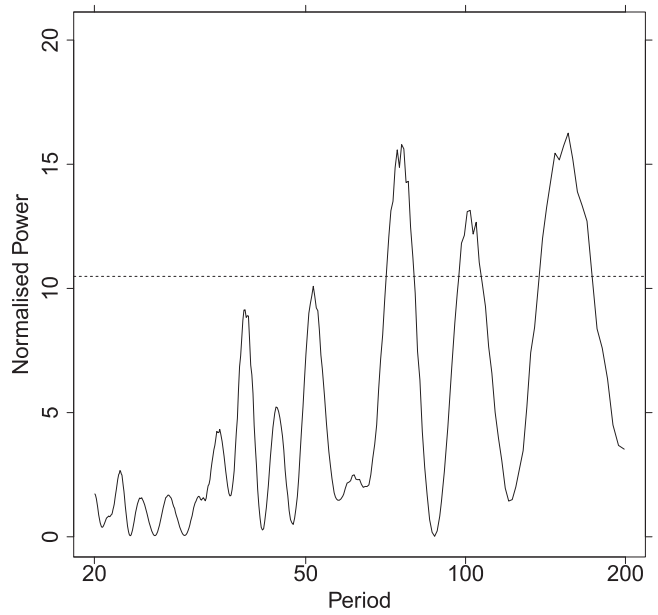

Figure 4. Lomb–Scargle periodogram of the pulse width at the 50% level with a cutoff level set at $p = 0.001$. Significant peaks are at periods of 78 ± 5, 100 ± 7, and 137 ± 12 days. Due to the discontinuity, data after the micro glitch at MJD $= 57143$ was excluded from this analysis.

occurring in the cone, whereas Vela (being a young pulsar) should have main core emission rather than conal emission (Rankin 1990).

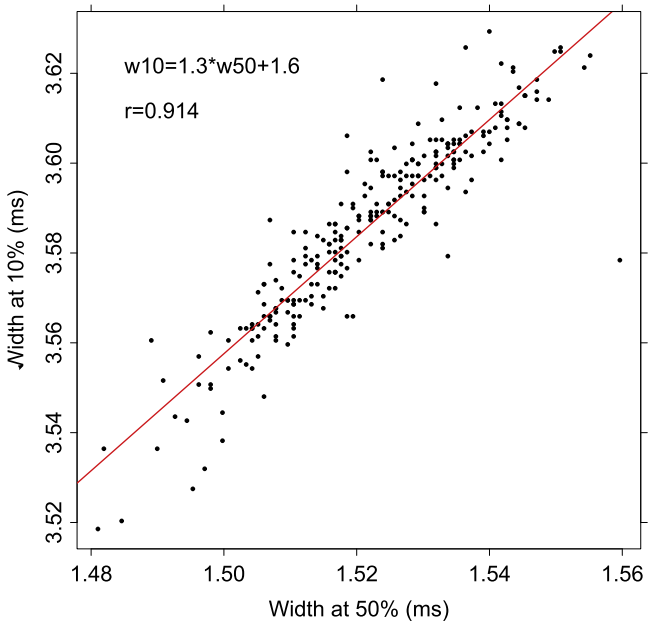

Figure 5. Correlation of the pulse width at 10% of the peak to 50% of the peak. Low S/N days have been removed.

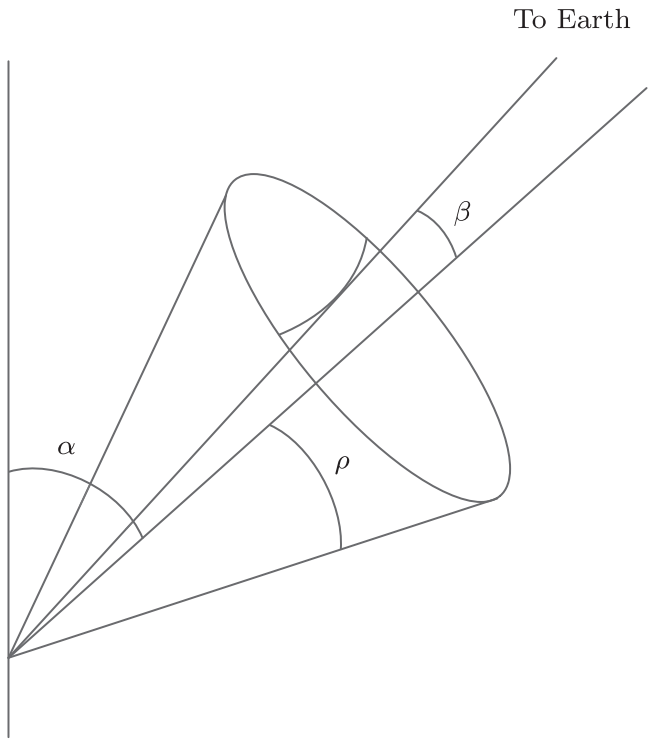

Figure 6. Simple graphic showing angles for the Vela pulsar where α is the angle between the rotational and magnetic axes (55°), β is the angle between the sight line and the magnetic axis (−6°), and ρ is the angular half-width of the emission cone (12°). See the text for references.

Finally, note in Figure 1(d) the 50 day "quiet time" just before the first micro-glitch and the gradual overall "settling" of the bright-pulse rate over time. This may settle to another "quiet time" which might indicate that another glitch is imminent.

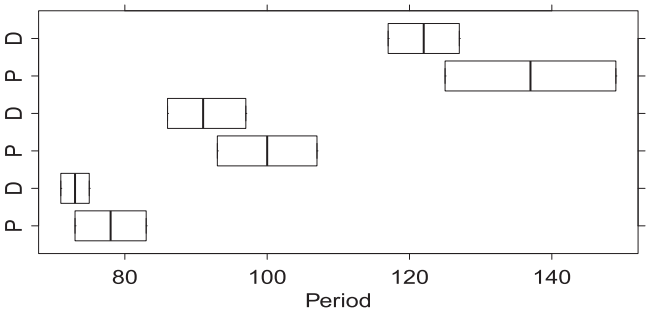

Figure 7. Periods (in days) from (P) our Lomb–Scargle plot (Figure 4) compared with the periods from the (D) X-ray observations from Durant et al. (2013).

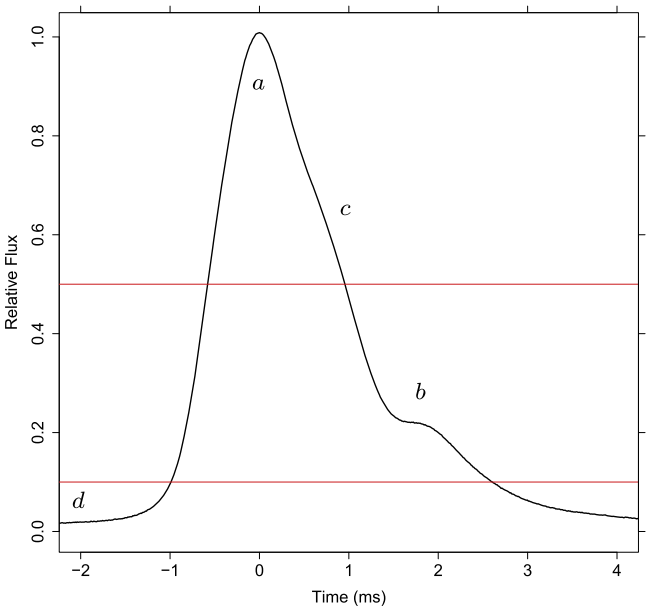

Figure 8. Typical daily integrated pulse profile (over 750,000 pulses) of J0835 −4510 at 1376 MHz showing the 10% and 50% levels. The letters *a, b, c,* and *d* label emission zones as discussed in Krishnamohan & Downs (1983). See the text.

4. CONCLUSIONS

We are carrying out an intensive single-pulse observation campaign of the Vela pulsar and have collected over 6000 hr of data. We have shown that the daily integrated pulse profile width changes both slowly over time and has a discontinuity after a micro-glitch. Bright-pulse rates are also shown to be affected by micro-glitches, but in an inconsistent manner.

We have found periodicities in the pulse width changes that match (within error bars) the exciting X-ray results from Durant et al. (2013) that imply free precession.

We hope that these results might shed some new light on the pulsar emission and glitching process, and to this end we intend to produce further papers from this large data set.

We would like to thank Mr. Brett Reid, Mr. Eric Baynes, Dr. Jamie McCallum, Mrs. Melissa Humphries, Dr. Andrew Cole, and Dr. Lucia Plank of the Department of Physical Sciences at the University of Tasmania who have cheerfully assisted us in the collection and analysis of this data. Professor Joanna Rankin also provided stimulating input into this work. We would also like to acknowledge the Tasmanian Partnership for Advanced Computing (TPAC) at the University of Tasmania with funding from the Australian Government through its NCRIS and RDSI programs for the use of the 2.3 PB storage facility, without which this project would not be possible.

REFERENCES

Cordes, J. M. 1978, ApJ, 222, 1006
Cordes, J. M. 1993, in ASP Conf. Ser. 36, Planets Around Pulsars, ed. J. A. Phillips, S. E. Thorsett, & S. R. Kulkarni (San Francisco, CA: ASP), 43
Cordes, J. M., Downs, G. S., & Krause-Polstorff, J. 1988, ApJ, 330, 847
D'Alessandro, F. 1995, PhD thesis, Univ Tasmania
Dodson, R., Lewis, D., & McCulloch, P. 2007, Ap&SS, 308, 585
Durant, M., Kargaltsev, O., Pavlov, G. G., Kropotina, J., & Levenfish, K. 2013, ApJ, 763, 72
Hobbs, G. B., Edwards, R. T., & Manchester, R. N. 2006, MNRAS, 369, 655
Hotan, A. W., van Straten, W., & Manchester, R. N. 2004, PASA, 21, 302
Jankowski, F., Bailes, M., Barr, E., et al. 2015, ATel, 6903, 1
Johnston, S., van Straten, W., Kramer, M., & Bailes, M. 2001, ApJL, 549, L101
Krishnamohan, S., & Downs, G. S. 1983, ApJ, 265, 372
Link, B., & Epstein, R. I. 1997, ApJL, 478, L91
Lomb, N. R. 1976, Ap&SS, 39, 447
Lorimer, D. R., & Kramer, M. 2004, Handbook of Pulsar Astronomy (Cambridge: Cambridge Univ. Press)
Manchester, R. N., Hobbs, G. B., Teoh, A., & Hobbs, M. 2005, AJ, 129, 1993
Palfreyman, J. L., Hotan, A. W., Dickey, J. M., Young, T. G., & Hotan, C. E. 2011, ApJL, 735, L17
Radhakrishnan, V., & Manchester, R. N. 1969, Natur, 222, 228
Rankin, J. M. 1990, ApJ, 352, 247
Rankin, J. M. 1993, ApJ, 405, 285
Reichley, P. E., & Downs, G. S. 1969, Natur, 222, 229
Scargle, J. D. 1982, ApJ, 263, 835
Stairs, I. H., Lyne, A. G., & Shemar, S. L. 2000, Natur, 406, 484
van Straten, W., & Bailes, M. 2011, PASA, 28, 1
Wright, G. A. E. 2003, MNRAS, 344, 1041